

Directional information from neuronal ensembles in the primate orofacial sensorimotor cortex

F. I. Arce,¹ J.-C. Lee,² C. F. Ross,¹ B. J. Sessle,² and N. G. Hatsopoulos^{1,3}

¹Department of Organismal Biology and Anatomy, University of Chicago, Chicago, Illinois; ²Faculty of Dentistry, University of Toronto, Toronto, Ontario, Canada; and ³Committees on Computational Neuroscience and Neurobiology, University of Chicago, Chicago, Illinois

Submitted 27 February 2013; accepted in final form 18 June 2013

Arce FI, Lee JC, Ross CF, Sessle BJ, Hatsopoulos NG. Directional information from neuronal ensembles in the primate orofacial sensorimotor cortex. *J Neurophysiol* 110: 1357–1369, 2013. First published June 19, 2013; doi:10.1152/jn.00144.2013.—Neurons in the arm and orofacial regions of the sensorimotor cortex in behaving monkeys display directional tuning of their activity during arm reaching and tongue protrusion, respectively. While studies on population activity abound for the arm motor cortex, how populations of neurons from the orofacial sensorimotor cortex represent direction has never been described. We therefore examined and compared the directional information contained in the spiking activity of populations of single neurons recorded simultaneously from chronically implanted micro-electrode arrays in the orofacial primary motor (MIO, $N = 345$) and somatosensory (SIO, $N = 336$) cortices of monkeys (*Macaca mulatta*) as they protruded their tongue in different directions. Differential modulation to the direction of tongue protrusion was found in >60% of task-modulated neurons in MIO and SIO and was stronger in SIO ($P < 0.05$). Moreover, mutual information between direction and spiking was significantly higher in SIO compared with MIO at force onset and force offset ($P < 0.01$). Finally, the direction of tongue protrusion was accurately predicted on a trial-by-trial basis from the spiking activity of populations of MIO or SIO neurons by using a discrete decoder ($P < 0.01$). The highly reliable decoding was comparable between MIO and SIO neurons. However, the temporal evolution of the decoding performance differed between these two areas: MIO showed late-onset, fast-rising, and phasic performance, whereas SIO exhibited early-onset, slow-rising, and sustained performance. Overall, the results suggest that both MIO and SIO are highly involved in representing the direction of tongue protrusion but they differ in the amplitude and temporal processing of the directional information distributed across populations of neurons.

orofacial sensorimotor cortex; motor cortex; somatosensory cortex; decoding; electrophysiology

PROPER TONGUE POSITIONING relative to other orofacial structures is important in facilitating daily activities such as feeding and speech. Biting one's tongue and having trouble articulating words are common human experiences, but impairment of orolingual function is also a serious component of several sensorimotor disorders of the orofacial system, including dysphagia (Ciucci et al. 2011; Fleming et al. 2012; Nuckolls et al. 2012), orofacial dystonia, dysarthria, and apraxia. The potential for tongue-task training in dysphagia rehabilitation (Kennedy et al. 2010; Konaka et al. 2010; Steele et al. 2010) and the demonstrated plasticity of sensorimotor cortex during tongue-

task training in human and nonhuman primates (Arce et al. 2011; Arima et al. 2011; Avivi-Arber et al. 2011; Sessle et al. 2005, 2007) make an understanding of cortical mechanisms of lingual motor control a subject of considerable interest.

The orofacial sensorimotor cortex has been implicated in the complex control of tongue and jaw movements (Lin et al. 1994a; Lowe 1980; Murray et al. 1991; Murray and Sessle 1992a; Sessle 2006; Yao et al. 2002). Such complex control relies on efficient processing of sensory inputs and motor outputs mediated by abundant anatomical interconnections between the orofacial primary motor cortex (MIO) and somatosensory cortex (SIO) (Hatanaka et al. 2005; Huang et al. 1989a, 1989b). In particular, neurons in MIO and SIO of monkeys have been shown to modulate their spiking activity to the direction of voluntary tongue protrusion (Lin et al. 1994b; Murray and Sessle 1992c). This is akin to the directionally tuned motor cortical neurons (Georgopoulos et al. 1982; Kalaska et al. 1989; Schwartz et al. 1988) and somatosensory cortical neurons (Burbard et al. 1991; Prud'homme and Kalaska 1994; Soso and Fetz 1980) of the arm region of the sensorimotor cortex when monkeys reach to different directions.

The advent of chronically implanted multielectrode arrays has accelerated research using analyses of simultaneous activity in neuron populations. This approach is based on the view that feature representations do not depend solely on the activity of single neurons but also rely on distributed patterns of activity across neuronal ensembles. One powerful use of population activity from neuronal ensembles has been in addressing the problem of decoding: given the concurrent activity of a population of neurons, how well can we predict a movement feature or a sensory event? Decoding movement features, such as direction of arm-reaching movements, has been successfully shown using spiking activities of populations of MI neurons (Georgopoulos et al. 1986; Hatsopoulos et al. 2004; Serruya et al. 2002; Taylor et al. 2002; Wessberg et al. 2000).

While there have been numerous studies on how the arm sensorimotor cortex encodes movement features through concurrent activity of populations of neurons, there have been no analogous studies in the orofacial sensorimotor cortex. Because of the bilateral structure of the tongue, the orofacial control system may not function identically to the limb control system. Moreover, nothing is known yet about how population coding of direction may differ between simultaneously recorded neuronal ensembles in MIO and SIO. Since MIO is directly concerned with movement generation while SIO provides sensory information to guide movement, the temporal dynamics of the population coding of directional information

Address for reprint requests and other correspondence: N. G. Hatsopoulos, Dept. of Organismal Biology and Anatomy, Committees on Computational Neuroscience and Neurobiology, Univ. of Chicago, 1027 East 57th St. Chicago, IL 60637 (e-mail: nicho@uchicago.edu).

may differ between these two cortical areas. In this study, we addressed this question by evaluating how well direction can be decoded on a trial-by-trial basis by using spiking activity of neurons recorded simultaneously from both Mlo and SIo as monkeys make voluntary tongue protrusions in different directions. Here we used a form of discrete decoder that decodes the discrete direction as opposed to continuous decoders used to decode instantaneous direction.

MATERIALS AND METHODS

All protocols for animal care and experimentation were submitted to and approved by the University of Chicago's Institutional Animal Care and Use Committee and complied with the National Institutes of Health *Guide for the Care and Use of Laboratory Animals* and the Canadian Council for Animal Care. Before, during, and after experimentation, monkeys were assessed regularly and assiduously for general well-being.

Behavioral Task

Two subjects [male *Macaca mulatta*; monkey B (10 kg) and monkey Y (12 kg)] were trained to protrude their tongue to apply force

on a transducer that was fixed in front of the animal in one of three directions (Fig. 1A), center, 30° left, or 30° right as measured relative to an imaginary line between the centers of the head and the mouth, as previously described (Murray et al. 1991; Murray and Sessle 1992c). Appropriate head and torso restraints were used to prevent head or trunk movements. Indeed, monkeys did not reorient their head and trunk to make the lateral tongue movements.

Each direction of tongue protrusion was performed in blocks of 100 trials. To achieve spatially distinct tongue protrusions, the force transducer (model 462-D3-2-10P1R, Revere Transducers, Tustin, CA) was positioned such that right- and left-side protrusions of the tongue occurred proximal to the angle of the mouth and bounded by the incisor teeth.

With the head fixed and the forearms restrained, the monkey sat in front of a computer screen that displayed the targets and the cursor, which represented the amplitude of tongue-protrusive force applied on the transducer. Two target windows were shown on the screen to indicate the required force range, i.e., a base target window with minimal tongue-protrusive force required (0–20 g) and a force target window with required tongue-protrusive force (70–90 g). Both base and force targets were always presented at the same position on the computer screen. Figure 1B describes the sequence of events in a trial. The trial started with the appearance of the cursor after an intertrial

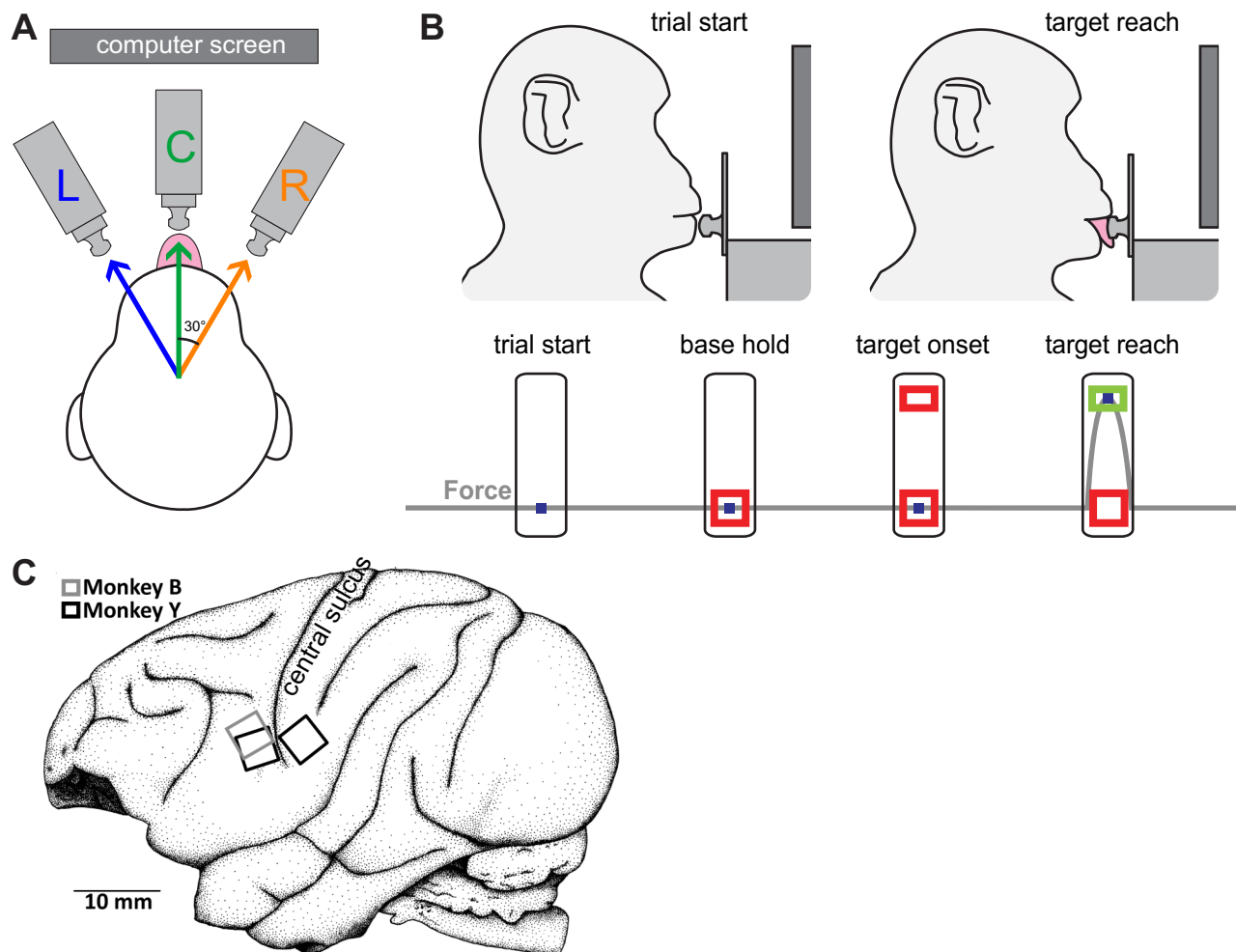


Fig. 1. Experimental setup and paradigm. A: diagram showing the 3 positions of the force transducer (gray-filled rectangle) placed in front of the monkey: center (C, green line), 30° right (R, orange line), and 30° left (L, blue line) relative to an imaginary line between the centers of the head and the mouth. Force transducer was positioned such that right- and left-side protrusions of the tongue occurred proximal to the angle of the mouth. B: sequence of events in a trial. The blue square represents the cursor, while the colored boxes represent the base and force targets. A plot of the amplitude of tongue-protrusive force associated with the cursor displacement is superimposed for illustration (gray line). C: location of orofacial primary motor (Mlo) and somatosensory (SIo) cortex arrays of monkey Y and monkey B.

interval (ITI) of 3 s. The base target appeared after a random period between 0.75 and 1.25 s after trial start to cue the monkey to keep the cursor within the base target window for a random hold period between 0.5 and 1 s. During this hold period, the monkey was allowed to keep the tongue touching the transducer or retracted. The monkeys behaved variably during the base hold period. These visually observed types of behavior could be one of the following: 1) the monkey kept the tongue in the oral cavity until the onset of the force target or 2) the monkey protruded the tongue at the appearance of the base target. If the monkey protruded the tongue for the base target, it either kept the tongue touching the transducer or retracted the tongue back and kept it in the oral cavity until the onset of the force target. Upon successful hold at the base target (i.e., the monkey did not move the cursor beyond the base target window), the force target appeared on the screen to signal the monkey to move the cursor into the force target window. When the cursor had reached the force target within the allotted time (5 s), the force target changed color to indicate success and the monkey immediately received a juice reward. Reward was delivered through a spout inserted through a tongue piece that was attached to the transducer. The trial end was defined by a success or failure event, and an ITI immediately followed during which the screen was blanked until the appearance of the cursor at the start of the next trial. Failure events included those events when the monkey did not meet the requirements for hold and movement times at either or both base and force targets. Aside from the visual cues, distinct audio cues also accompanied the following events: trial start, appearance of base and force targets, and success.

The behavioral program was written with Spike2 software (Cambridge Electronic Design, Cambridge, UK). Force transducer signals and the behavioral event logs and timestamps were recorded at 2 kHz and stored with the Power 1401 data acquisition system (Cambridge Electronic Design). User-designed pulse signals were generated to mark behavioral events and were sent to the neural data acquisition systems for off-line synchronization of timestamps across the different data acquisition systems.

Electrophysiology

Under general anesthesia, each monkey was chronically implanted with two silicon-based microelectrode arrays of 100 electrodes (BlackRock Microsystems, Salt Lake City, UT) in the MIO and SIO of the left hemisphere (Fig. 1C). The microelectrodes on the array were separated from their immediate neighbors by 400 μm , and their length was 1.0 mm for all implanted arrays except for one array, which was 1.5 mm in length (MIO of *monkey Y*). Microelectrode tips were coated with iridium oxide. Surgical details have been described previously (Rousche and Normann 1998). Implantation sites were verified on the basis of surface landmarks and observed evoked responses from the tongue and fingers following monopolar surface stimulation of MIO (50 Hz, 200- μs pulse duration, 2–5 mA) during the surgical procedure. SIO was defined as the region posterior to the central sulcus and below the tip of the intraparietal sulcus and at the same longitudinal axis with MIO. During task training after the monkeys had recovered from surgery, intracortical microstimulation (ICMS) was also applied to the implanted microelectrode array. ICMS-evoked motor activities confirmed appropriate array implantation. During each recording session, signals were amplified (gain 5,000 \times), band-pass filtered (0.25–7.5 kHz), and recorded digitally (14 bit, 30 kHz) from both arrays simultaneously with two Cerebus acquisition systems (BlackRock Microsystems). Spike waveforms that passed a user-defined threshold were stored and sorted off-line with Offline Sorter (Plexon, Dallas, TX). Data from array channels with no signal or with large amounts of 60-Hz line noise were excluded. We collected a total of five data sets from MIO (4 from *monkey Y* and 1 from *monkey B*) and four data sets from SIO of *monkey Y*. A data set is defined as the simultaneously recorded neural signals from one array during a single recording session when the monkey completed at least one block of

100 trials of tongue protrusion for each of the three transducer positions. These data sets were collected after each monkey had previously undergone 9–12 wk of training on the task but limited to tongue protrusions in the center direction. Prior to data collection, monkeys were given training trials on right and left tongue protrusions.

Electromyograms

Two weeks after array implantation surgery, monkeys were also chronically implanted with fine-wire electromyography (EMG) electrodes (2 nickel-chromium alloy fine wires of 0.05-mm diameter) placed subcutaneously in the masseter, genioglossus, geniohyoid, and anterior digastric muscles of both sides of the face. Electrode placement was verified upon visual observation of muscle twitches evoked by electrical stimulation (600-ms train of 5-ms pulses delivered at 60 Hz). EMG signals were amplified (50–5,000 \times), band-pass filtered (10–300 Hz; Grass Technologies, West Warwick, RI), and digitized at 2,000 Hz with the Cerebus acquisition system. EMG data were collected while ICMS was applied to neural recording sites in MIO and SIO (see Fig. 1), but collection was no longer viable at the time of data collection for tongue protrusions to different directions.

Sensory and Motor Maps

Both sensory and motor mappings were performed on awake and behaving monkeys without using any form of sedation. Mechanoreceptive field (RF) properties of recorded neurons from MIO and SIO were identified by applying mechanical stimuli (by a gloved finger) to the skin on both sides of the orofacial structures (i.e., cheeks, upper and lower lips). A cotton swab was also used to stimulate the middle portion of the dorsum of the tongue; discrimination between a RF on the left vs. right side of the tongue was not possible since tongue position could not be fixed during sensory stimulation in an awake animal. To identify motor maps, ICMS applied to the implanted microelectrode arrays was carried out routinely (UC Stimulator, Sigenics, Chicago, IL) with protocols described in previous studies of MIO and SIO (Huang et al. 1989a, 1989b; Murray and Sessle 1992a). For MIO, we used high-frequency short-train monophasic stimulation (cathodal 333 Hz, 12 pulses/train, 0.2-ms pulse duration, 2.8-ms interpulse duration), which these previous studies have shown is effective in evoking muscle twitches or elementary movements (e.g., tongue protrusion, jaw opening). For SIO, we used low-frequency long-train monophasic stimulation (50 Hz, 100 pulses/train, 0.2-ms pulse duration, 19.8-ms interpulse duration), which previously has been shown to be effective in evoking semiautomatic movements of chewing and swallowing (Huang et al. 1989a; Martin et al. 1999). Maximal current applied was 30 μA . ICMS threshold intensities that evoked twitches of tongue and facial muscles, tongue protrusion, and jaw movements ranged from 5 to 30 μA .

Videofluoroscopy

Prior to chronic implantation of the multielectrode arrays, the monkeys were implanted with up to six 0.5-mm-diameter spherical tantalum markers in the midline of the anterior, middle, and posterior thirds of the tongue. We collected two-dimensional tongue kinematics by using fluoroscopy combined with a high-speed motion camera (Xcitex, Cambridge, MA). Data were collected while monkeys performed tongue protrusions to the center direction only (100 frames/s) and simultaneously with neural recordings. Positions of tongue markers were digitized off-line and synchronized with the times of behavioral events (e.g., trial start, target onsets, reward) and neural events.

Data Analysis

Behavioral analysis. Only successful trials, i.e., trials in which the monkeys were able to apply the required force at each force target

within the allotted time, were used in all analyses. Trials were further selected on the basis of similarities of force profiles across all directions of tongue protrusion in a data set. Onsets of tongue movement and force generation were marked when tongue velocity/force last exceeded a defined threshold (1 mm/s or 1 g) prior to reaching two-thirds of peak velocity/force (Arce et al. 2009). Force offset was defined as the time when force reached 1 g after reaching peak force.

Neural analysis. We analyzed single-unit activity recorded from Mlo (monkey Y: 67–86 units/data set, monkey B: 34 units) and Slo (monkey Y: 80–86 units/data set) related to two epochs during a trial, i.e., preparatory (600 ms prior to force onset) and movement (600 ms after force onset). Single units were deemed task-modulated when their firing rates during a hold period (500 ms prior to force target onset) differed significantly from firing rates during the preparatory or movement epochs (paired *t*-test, $P < 0.01$). To evaluate the degree of task-modulation, we calculated a modulation index as

$$\text{Modulation index} = \frac{r_{(B,t)} - r_{(A,t)}}{r_{(A,t)}} \quad (1)$$

where r is the mean firing rate during A (hold period) or B (preparatory or movement epoch) of trial t . The activity of each task-modulated neuron was then assessed for modulation to the direction of tongue protrusion by comparing firing rates during the preparatory or movement epoch across all directions by one-way analysis of variance (ANOVA, $P < 0.05$). A directional index was calculated for neurons that showed significant rate modulation to the direction of tongue protrusion as Directional index = max(Modulation index) – min(Modulation index). A preferred direction (PD) was described for neurons with firing rates that were significantly higher from the two other directions of tongue protrusion (ANOVA post hoc Tukey–Kramer correction for multiple comparisons, $P < 0.05$).

We also quantified the amount of directional information available in the neuronal response with information theoretic methods (MIToolbox; Brown et al. 2012). Mutual information (Shannon 1948) between the spiking of single neurons (X) and the direction of tongue protrusion (Y) was estimated as a reduction of the entropy of the observed spiking, $H(X)$, given the entropy of observed spiking conditioned on the direction of tongue protrusion, $H(X|Y)$,

$$I(X, Y) = H(X) - H(X|Y) \quad (2)$$

$H(X)$ is the Shannon entropy defined for each neuron's spike count, X , measured in a 100-ms time bin as

$$H(X) = -\sum_{k=1}^N p_k \log_2(p_k) \quad (3)$$

where N is the maximum number of spike counts ($N = 11$) and p_k is the probability of observing k spikes in the bin. $H(X|Y)$ is the conditional entropy and is defined as

$$H(X|Y) = -\sum_y p(y) \left[\sum_x p(x|y) \log_2 p(x|y) \right] \quad (4)$$

Marginal and conditional probabilities were estimated empirically. To account for biases in the estimation, we estimated the mutual information by randomly shuffling the direction labels associated with each trial (100 shuffles) and subtracting the mean shuffled estimates from the mutual information obtained from the actual data.

In this study, mutual information quantifies the reduction in uncertainty of the response of a single neuron given knowledge of the direction of tongue protrusion. Equivalently, it quantifies the reduction in uncertainty of tongue direction given knowledge of the response of a single neuron. Thus it gives a measure of the strength in the relationship between the spiking activity and the direction of tongue protrusion. Moreover, by examining binned neuronal data aligned at specific behavioral events, we were able to compare the amplitudes and temporal evolution of the mutual information between the two cortical areas.

Decoding direction of tongue protrusion using spiking activity. A K -nearest-neighbor classifier (KNN) was used to evaluate the ability of spiking activity from a population of simultaneously recorded Mlo and Slo neurons to predict the discrete direction of tongue protrusion on a trial-by-trial basis. KNN is a nonparametric learning algorithm that classifies objects based on the closest training examples in the feature space. We used Euclidean distance to identify K nearest neighbors. The choice of $K = 9$ as the number of nearest neighbors was made considering the size of our smallest training data set ($n = 84$) and after determining that other K s yielded similar results ($K = 7$ or $K = 10$). Each feature dimension corresponded to the spike counts for each neuron measured in a 100-ms window. Classification was repeated for different 100-ms windows incremented in 5-ms steps. We used a fixed number of test trials ($N = 8$) based on classifier training trials whose number varied per data set (Y1–Y4: $N = 62, 28, 62, 32$; B1: $N = 62$). The performance of the classifier was evaluated based on the percentage of correct classifications of the test trials. For validation, we ran the algorithm 100 times, using a different set of randomized test and training trials for each run. To assess the reliability of decoding, we used a binomial test at $P < 0.01$ significance level.

RESULTS

The displacement of the tongue in each monkey during tongue protrusion to a center direction, as captured by videofluoroscopy (Fig. 2A), showed that each monkey's tongue approached the transducer along a straight axis between the center of the force transducer and the middle portion of the tongue and applied force on the transducer with the anterior portion of the tongue. Figure 2B shows tongue trajectories, corresponding vertical and horizontal displacements, and velocities during central tongue protrusions. Tongue trajectories were typically straight with bell-shaped velocities (Fig. 2B, top). Tongue velocities dropped as the tongue approached the transducer. After transducer contact, horizontal and vertical displacements were minimal as the monkey applied force on the transducer until the required force was reached as signaled by the reward cues (Fig. 2B, bottom). Upon receiving the juice reward, the monkey started to release the force by retracting the tongue. While single-plane videofluoroscopy could not yield accurate kinematic data during oblique tongue protrusions (i.e., right and left directions), visual observation and video recordings suggested that both monkeys used the same strategy as described above for central tongue protrusions.

Reaction times measured from the onset of the force target to the onset of force generation had a median of 0.6 s (Fig. 2C) and ranged between -0.04 and 4.7 s. Previous studies have reported comparable mean reaction times for tongue protrusion (Murray et al. 1991; Murray and Sessle 1992b). The negative values signify that monkeys applied force on the transducer prior to the onset of force target, suggesting that the tongue was already touching the transducer prior to target onset. The longer reaction times are due to the fact that monkeys were given up to 5 s to start applying force on the transducer. Reaction times did not differ across directions (ANOVA, $P > 0.10$).

Spike Modulation to Direction of Tongue Protrusion

Over 70% of neurons recorded in the left sensorimotor cortices showed modulation of their preparatory and/or movement-related activity to the task of tongue protrusion (Table 1, task-modulated neurons); their mean firing rates relative to the hold period changed significantly prior to or during the gener-

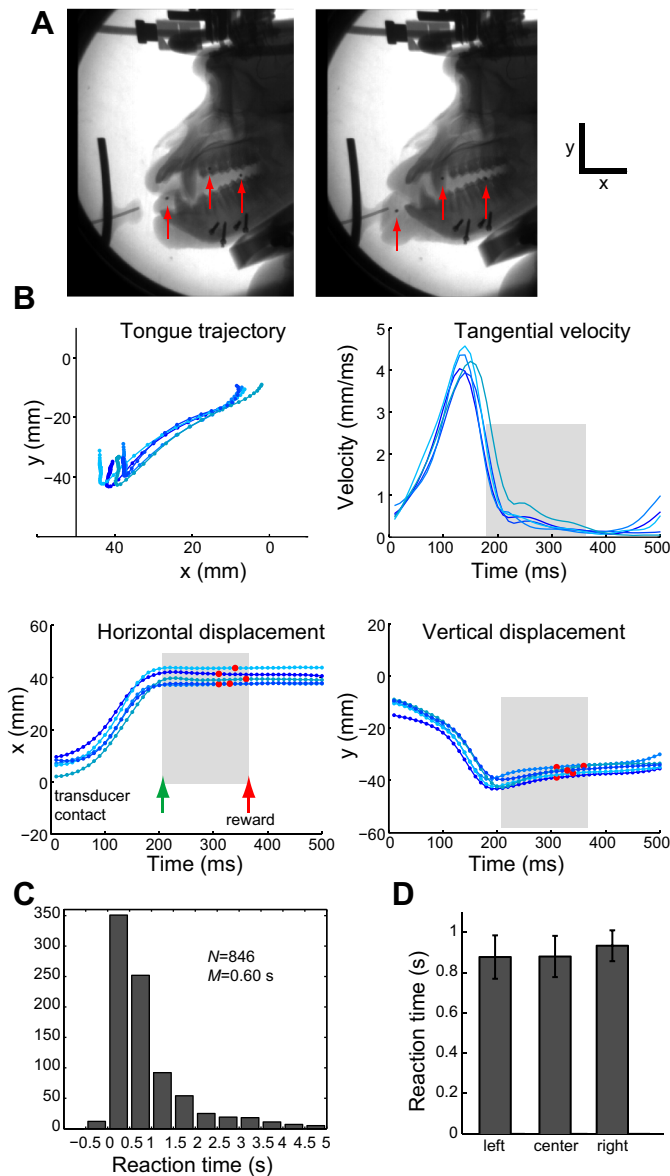


Fig. 2. Kinematics of tongue protrusion. *A*: videofluoroscopic images of the monkey at the start and end of tongue protrusion, with red arrows added to show the location of 3 spherical tantalum tongue markers. *B*: single-trial trajectories, horizontal and vertical displacements of the tongue, and corresponding velocities from the onset of tongue protrusion to reward. Shaded gray area shows the period during force generation that was monitored by the force transducer from transducer contact (green arrow) to reward (red arrow and red dots on individual displacement plots). *C*: histogram of reaction times measured from force target onset to force onset for all data sets combined. N = number of trials, M = median. *D*: reaction times as a function of the direction of tongue protrusion.

ation of tongue-protrusive force (paired t -test, $P < 0.01$). Figure 3 illustrates the perievent time histograms (PETHs) of MIO and SIO neurons recorded simultaneously in one session. These task-modulated neurons exhibited varying firing patterns; while peak activity of two MIO neurons shown in Fig. 3, *A* and *B*, occurred on or before force onset, peak activity of the MIO neuron shown in Fig. 3*C* occurred at peak force when the required force level was achieved (Fig. 3, *G* and *H*). In Fig. 3, *D* and *E*, SIO neurons showed peak activity coincident with peak force, while the SIO neuron shown in Fig. 3*F* was mostly

active prior to force onset. The firing activity of all MIO and SIO neurons plotted in Fig. 3 showed marked differences across the directions of tongue protrusion. Of these task-modulated neurons, $>60\%$ showed differential modulation to the direction of tongue protrusion during the preparatory epoch [Fig. 4*A*; SIO: $69(\pm 9)\%$, MIO: $60(\pm 14)\%$, ANOVA, $P < 0.05$] and/or movement epoch [SIO: $77(\pm 4)\%$, MIO: $65(\pm 9)\%$, ANOVA, $P < 0.05$]. The differences in spiking activity across directions of tongue protrusion were not attributable to differences in the tongue-protrusive force, as mean force profiles were not significantly different across the three directions (see Fig. 3, *G* and *H*). This was true for all data sets (data not shown). Moreover, a large proportion of directionally modulated neurons in both MIO and SIO (Fig. 4*B*) exhibited a preferred direction (PD), the direction in which the firing rate was significantly higher from the other two directions (ANOVA post hoc, $P < 0.05$). The proportions of neurons with PD were comparable for both cortical areas (Fig. 4*B*; binomial test, $P > 0.1$). Figure 4, *C* and *D*, show the distribution of PDs for preparatory and movement-related activity. In MIO, the peak of the distribution was for left protrusions for both preparatory and movement epochs (binomial test, $P < 0.05$). In contrast, the peak of the distribution in SIO was for right protrusions for the preparatory epoch (binomial test, $P < 0.05$). For the movement epoch, proportions were not significantly different between left and right protrusions (binomial test, $P > 0.10$). Using a directional index, we compared the depth of directional modulation between the preparatory and movement epochs of directionally modulated neurons within and across cortical sites. In both MIO (t -test, $P > 0.1$ for all data sets) and SIO (t -test, $P > 0.1$ for all data sets except Y3, $P < 0.01$), directional indexes between preparatory and movement epochs of neurons were comparable. Comparing cortical sites, directionally modulated SIO neurons exhibited stronger directional modulation than MIO neurons during both preparatory (Fig. 4*E*; t -test, $P < 0.01$) and movement (Fig. 4*F*; t -test, $P < 0.05$) epochs.

We also performed the above-mentioned analyses by using neural activity aligned at force target onset. The activity of MIO and SIO neurons from target onset to 0.5 s after showed significant task-modulation (paired t -test, $P < 0.01$). However, the proportion of task-modulated neurons in both MIO and SIO was significantly lower for neural activity aligned at target onset (MIO: 46.7 ± 5.3 , SIO: 39.5 ± 12.7) than the proportion for activity during the “preparatory epoch” aligned at force onset (MIO: 77 ± 3.5 , SIO: 64 ± 10.1 , binomial test, $P > 0.1$). Similarly, there were significantly fewer directionally modulated neurons for neural activity aligned at target onset (MIO: 20.7 ± 4.8 , SIO: 19.1 ± 6.1) than for activity during the “preparatory epoch” aligned at force onset (MIO: 60.3 ± 6.2 , SIO: 68.9 ± 4.3 , binomial test, $P > 0.1$). These results suggest that the neural activity of MIO and SIO neurons is better time-locked to the force onset compared with the target onset, and thus may signal more reliably the coding of force onset rather than the target onset.

Neuronal Mechanoreceptive Fields and ICMS-Evoked Responses

Many of the directionally modulated MIO neurons exhibited RFs that were restricted to the middle portion of the dorsum of the tongue; no response was elicited when tactile stimulation

Table 1. Proportion of task-modulated and directionally modulated neurons in Mlo and Slo

	Y1		Y2		Y3		Y4		B1	
	Mlo	Slo	Mlo	Slo	Mlo	Slo	Mlo	Slo	Mlo	Slo
Unit no.	67	85	79	86	79	80	86	85	34	
DM1/TM1	40/58	54/72	29/52	37/59	42/63	32/53	26/68	24/31	18/25	
DM2/TM2	45/60	54/68	38/61	53/67	40/63	57/71	34/65	17/24	22/31	
SNR	3.8	3.2	3.7	2.9	3.8	3.2	3.2	2.9	3.7	

Details of proportion of task-modulated neurons (TM) in orofacial primary motor cortex (Mlo) and orofacial somatosensory cortex (Slo) whose spiking activity was differentially modulated to the direction (directionally modulated, DM) of tongue protrusion in the preparatory (DM1/TM1) and movement (DM2/TM2) epochs. The medians of the signal-to-noise ratio (SNR) of the spike waveforms in each area per data set are also included. Values are shown for 4 data sets from monkey Y (Y1–Y4) and 1 from monkey B (B1).

occurred on the surrounding orofacial structures. We found a significant overlap between the neurons’ directional modulation and RF properties (Fig. 5A). Across data sets, the proportion of directionally modulated Mlo neurons that had tongue RFs was $72 \pm 7\%$ (i.e., 34 ± 2 of 48 ± 2 Mlo neurons that showed modulation to direction in either preparatory or movement epoch). This was significantly higher than the probability of a task-modulated neuron having a tongue RF ($63 \pm 2\%$), thus indicating a relationship between tongue RFs and modulation to the direction of tongue protrusion (Fig. 5B; binomial test, $P < 0.01$). For the simultaneously recorded Slo neurons, we were only able to test the RFs of Slo neurons recorded at 28 electrodes. From these 28 electrodes, there were 19 ± 3 Slo neurons (across all Slo data sets) that showed modulation to direction in either the preparatory or movement epoch and all

of them had a tongue RF (Fig. 5A), suggesting a very strong relationship between tongue RF and directional modulation (Fig. 5C; binomial test, $P < 0.001$). These directionally modulated Slo neurons also exhibited RFs involving other orofacial structures (i.e., upper and lower lips, cheek) that were predominantly bilateral and composite (Fig. 5D). Since it was not possible to measure RFs restricted to the left or right side of the tongue, how RFs in different parts of the tongue might be related to the neuron’s PD could not be assessed.

ICMS was carried out at some neuron recording sites to determine whether evoked motor activity was associated with neurons having tongue protrusion-related activity as previously described (Lin et al. 1994b; Murray and Sessle 1992c). ICMS of Mlo evoked muscle twitches of the left and/or right genioglossus (9 sites). Directionally modulated

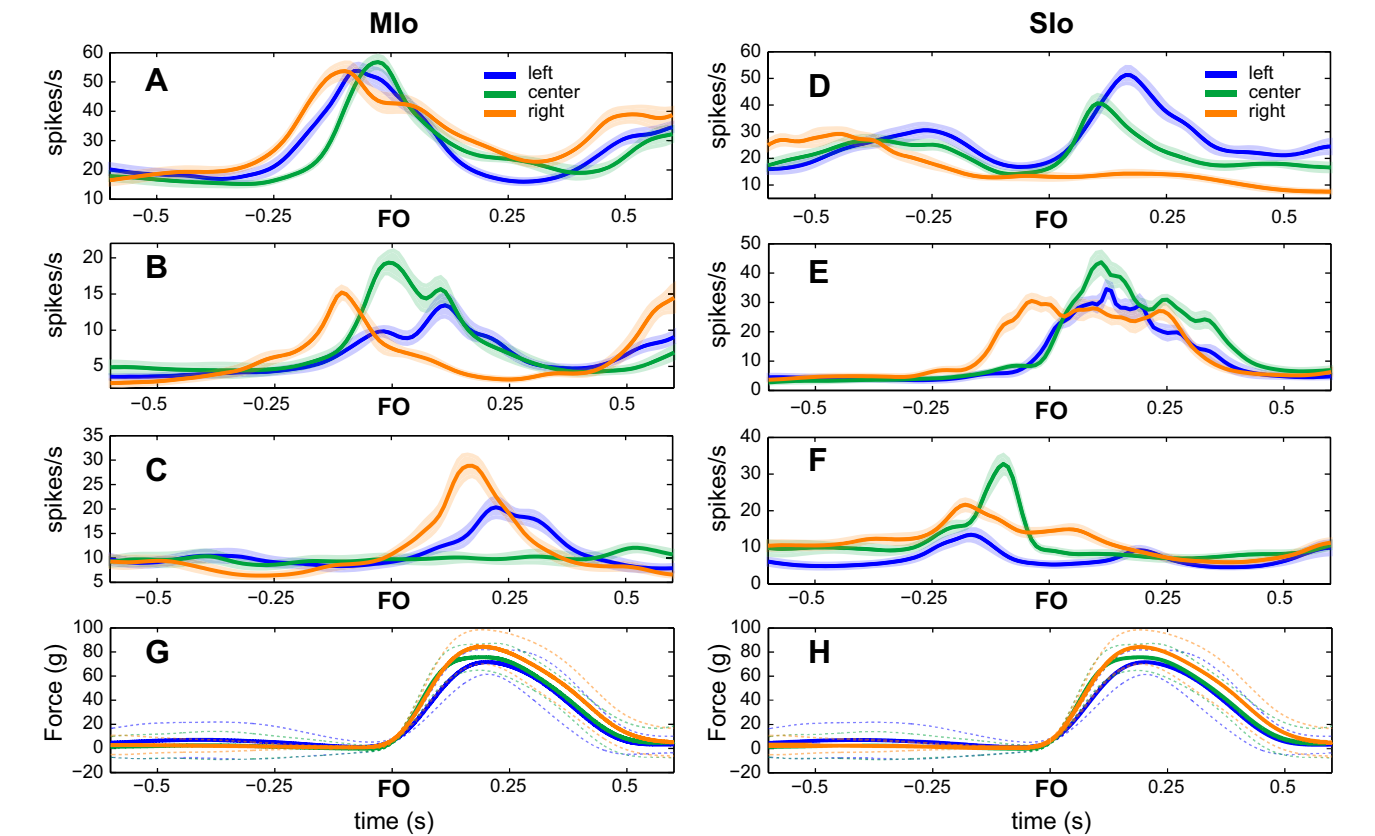


Fig. 3. Modulation of single-unit activity in relation to the direction of tongue protrusion. A–F: the diversity of activity patterns of single units as reflected in perievent time histograms (PETHs and ± 1 SE), smoothed by a 50-ms Gaussian kernel, show mean discharge of simultaneously recorded Mlo (A–C) and Slo (D–F) neurons while monkeys performed a task of tongue protrusion in three directions (left, center, right). PETHs are centered on force onset (FO). G and H: mean (solid lines) force profiles corresponding to the same trials used to plot the PETHs. Dashed lines correspond to ± 1 SE of the mean force profiles.

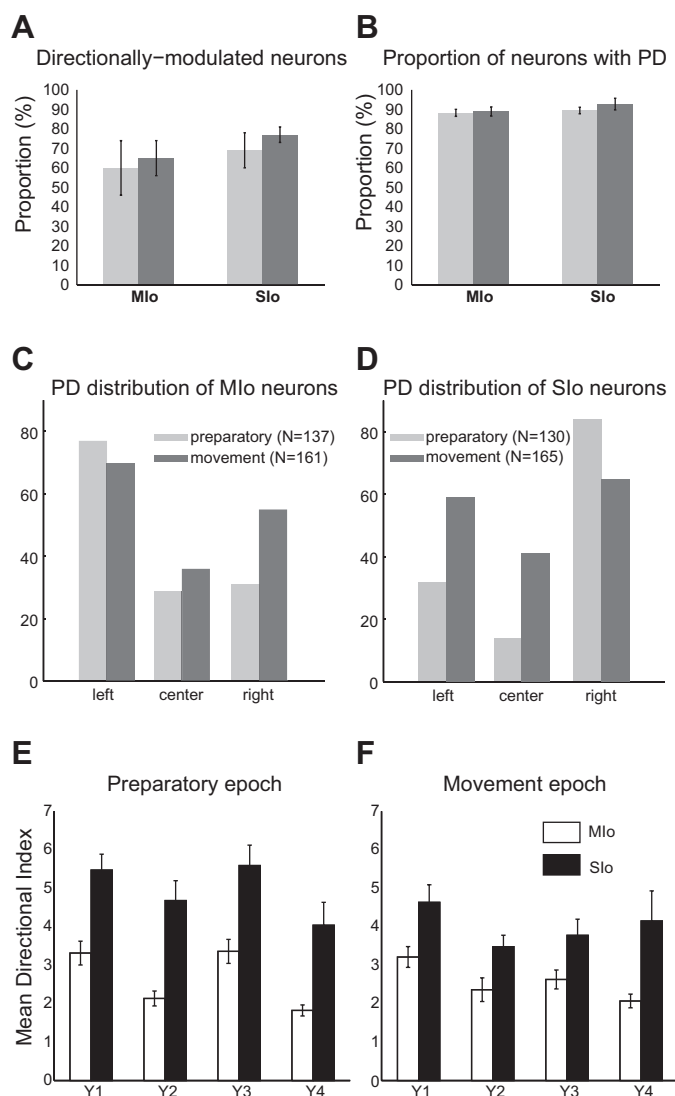


Fig. 4. Population profile of directionally modulated neurons in the orofacial sensorimotor cortices. *A*: proportion of directionally modulated neurons in Mlo and Sio. *B*: proportion of neurons in *A* that exhibited a preferred direction (PD) shown as mean (± 1 SE) across all data sets. *C* and *D*: histograms showing the distribution of PDs of Mlo and Sio neurons, respectively, in *B*. *E* and *F*: mean (± 1 SE) directional indexes of the preparatory (*E*) and movement-related (*F*) activity of neurons in *A* shown for each Mlo and Sio data set recorded simultaneously from monkey *Y* (Y1–Y4).

Mlo neurons were recorded from these ICMS sites. Since ICMS produced muscle twitches in both genioglossi in seven of nine sites, no attempt was made to relate the evoked responses to the Mlo neuron's PD because the direction of tongue protrusion could not be determined. ICMS in Sio evoked complex tongue movements from 22 sites. The tongue movements evoked at Sio sites were center or right protrusions either with or without jaw movements. Directionally modulated neurons were recorded in 91% ($n = 20$) of Sio sites, and $44(\pm 6)\%$ of these neurons had a PD that matched the direction of the ICMS-evoked tongue protrusions. For each data set and epoch, the proportion of ICMS-evoked tongue movements that matched the PD of the Sio neurons reached statistical significance in only three of eight instances (4 data sets $\times 2$ epochs, binomial test, $P < 0.05$).

Mutual Information Between Spiking Activity and Direction of Tongue Protrusion

Single neurons in Mlo and Sio showed significant increases in directional mutual information around the onset of tongue-protrusive force (Fig. 6, *A* and *B*), indicating that there were systematic changes in spiking activity with respect to the direction of tongue protrusion. Figure 6, *C* and *D*, show the mean mutual information aligned at force onset and force offset, respectively, across all neurons in Mlo or Sio recorded in each single session. Peak values of the mean mutual information in Mlo across all data sets were consistently observed around force onset (Fig. 6*C*, left). In contrast, peak values of the mean mutual information in Sio varied across data sets (Fig. 6*C*, right). Nevertheless, mutual information values corresponding to -100 ms to 100 ms relative to force onset were significantly higher in Sio than in Mlo (Fig. 6*C*; t -test, $P < 0.01$). Comparison between the distributions of the times when peak mutual information was observed in Mlo and Sio neurons revealed that the proportion of Mlo and Sio neurons with peak times at force onset was comparable (Fig. 7*A*; binomial test, $P > 0.1$); however, there were more Mlo neurons whose mutual information peaked 100 ms prior to force onset (Fig. 7*A*; binomial test, $P < 0.05$).

In two Sio data sets in Fig. 6*C*, we noted sustained levels of mutual information until 500 ms after force onset, corresponding to the time of force offset. This was, however, not observed in Mlo, where mutual information consistently dropped after force onset until force offset. This was confirmed when we estimated the mutual information for data aligned at force offset instead (Fig. 6*D*): Mlo neurons exhibited a $\sim 50\%$ drop in mutual information at force offset. This was not the case with Sio neurons, which showed increased, sustained, or $< 50\%$ decreased directional information. Indeed, mean mutual information at force offset was significantly higher in Sio than in Mlo (Fig. 6*D*; t -test, $P < 0.01$). Moreover, the distributions of time-to-peak mutual information corresponding to data aligned at force offset showed that the proportion of Sio neurons was significantly higher than that of Mlo neurons at force offset (binomial test, $P < 0.05$; Fig. 7*B*). This was consistent in the significantly higher number of Sio neurons that exhibited peak mutual information 0.5 – 0.6 s after force onset (Fig. 7*A*). We also observed a significantly low proportion of Sio neurons that had peak mutual information 0.3 s before force offset (Fig. 7*B*) and 0.3 s after force onset (Fig. 7*A*). This time corresponds roughly to the beginning of force release and reward.

Decoding Direction of Tongue Protrusion from Spiking Activity

We evaluated the ability of simultaneously recorded Mlo and Sio neurons to predict the direction of tongue protrusion on a trial-by-trial basis by using a nearest-neighbor rule to classify single trials into one of three directions of tongue protrusion. For data aligned at force onset, the activity of separate populations of Mlo and Sio neurons was shown to decode the direction of tongue protrusion reliably across all data sets (Fig. 8; binomial test, $P < 0.01$). Performance of the classifier reached a maximum of $> 85\%$ correct predictions for both Mlo and Sio, with their peaks being coincident starting around 200 ms prior to force onset (line *a* in Fig. 8*A*). However, the temporal profile of the classifier's performance showed marked differences be-

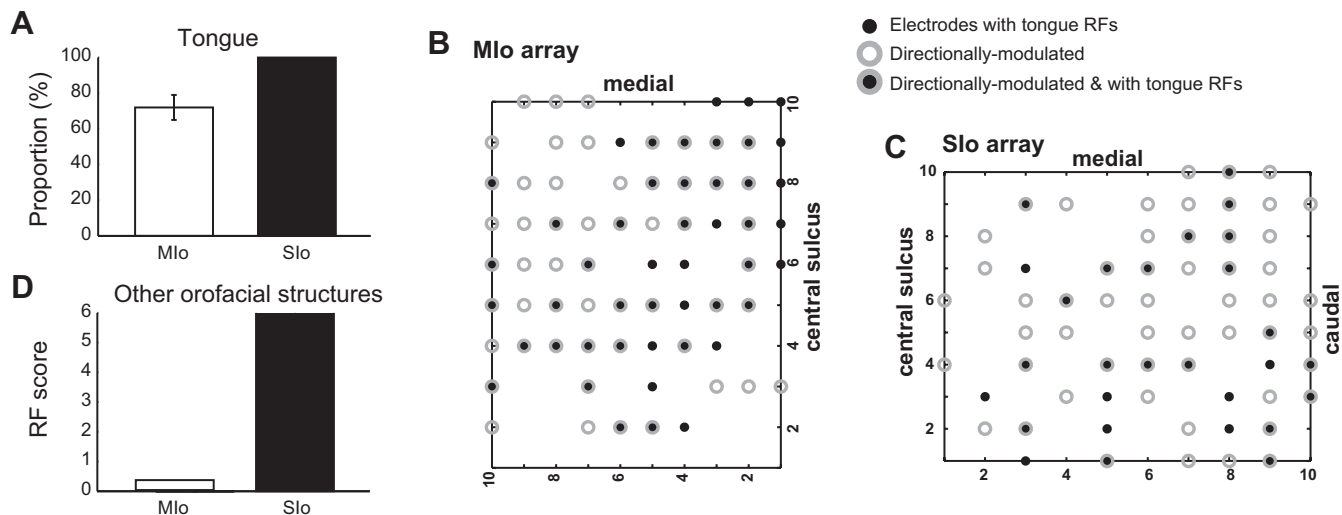


Fig. 5. Receptive field (RF) properties of Mlo and Sio neurons. *A*: proportion of directionally modulated neurons in Mlo and Sio that had tongue RFs. *B* and *C*: location of electrodes in the array where directionally modulated neurons and neurons with tongue RFs were recorded from the Mlo and Sio arrays, respectively. *D*: RF score of neurons in *A*. Each level corresponds to a unilateral orofacial structure ($N = 6$, upper and lower lips, cheeks of right and left face). Mlo neurons did not respond to tactile stimulation of other structures, while Sio neurons responded to all structures on both sides.

tween the two populations. First, the temporal evolution of directional information in Mlo exhibited a fast rise starting around 400 ms prior to force onset. In contrast, the temporal evolution of directional information in Sio showed a slower rise to peak. Second, the decoding performance for Sio neurons reached $P < 0.01$ significance level around 200 ms earlier than that of Mlo, thus indicating prior availability of directional information in Sio. Third, directional information in Mlo quickly dropped by the beginning of force release (*line c* in Fig. 8*A*), and decoding performance became unreliable by force offset (*line d* in Fig. 8*A*). In contrast, reliable decoding performance in Sio was maintained, indicating that directional information was sustained well beyond force offset (compare *lines c* and *d* in Fig. 8, *A* vs. *B*). Such differences cannot be attributed to the consumption of the reward, as swallowing could not have occurred during the time segment in which classifier performance of Mlo and Sio differed. Indeed, tongue kinematics collected during center tongue protrusion showed no significant change in both horizontal and vertical positions of the tongue 150–300 ms after the onset of reward signal (Fig. 2*B*). After force offset, we observed a return to reliable decoding performance in Mlo, corresponding to the time when tongue retraction occurred. Decoding performance in Mlo at this period was weaker compared with earlier periods corresponding to tongue protrusion and force generation. These results are consistent with the observed mutual information values in Mlo during these behavioral events (Fig. 6, *C* and *D*).

The temporal evolution of the decoding performances of *monkey B* and *monkey Y* showed important similarities: 1) fast rise from nonsignificant correct classification to highly reliable classification occurring at -0.4 s to force onset, 2) peak correct classification at -0.2 s to force onset, and 3) decoding performance becoming unreliable by force offset. Indeed, correlation analyses between the decoding performances of *monkey B* and *monkey Y* yielded high correlation coefficients ($R = [0.86, 0.67, 0.86, 0.85]$) and were highly significant ($P < 0.000001$). Although the temporal profiles were highly similar between the two monkeys, some differences in the amplitudes of the classification performance can be noted from -0.2 s to force onset

until 0.4 s after force onset: directional information in *monkey B* gradually dropped from peak performance, while that in *monkey Y* stayed high until 0.2 s after force onset. Nevertheless, we still found significant correlation between *monkey B* and *monkey Y* in three of four data sets from -0.2 s to force onset until 0.4 s after ($R = [0.46, 0.15, 0.40, 0.32]$, $P < 0.001$). This confirms that the difference between monkeys is not due to a difference in temporal profile shape but rather due to a difference in magnitude. Differences in the responses of the population of neurons recorded from the two monkeys (due to array location, quality of signal recording, etc.) may partially account for the different amplitudes in the classifier performance. Behaviorally, we found highly similar mean force profiles between the two monkeys (Pearson correlation, $P < 0.001$). However, we found shorter reaction times of *monkey B* compared with *monkey Y* (rank sum test, $P < 0.05$), and *monkey B* reached the required target faster than *monkey Y* in two data sets (rank sum test, $P < 0.05$). These behavioral differences may have contributed to the observed difference in classification performance.

We also performed the classifier analyses on neural data aligned at the onset of force target. For Mlo, the performance of the classifier showed a trend of increasing correct classification from target onset; however, it did not reach significant levels (Fig. 8*C*; binomial test, $P > 0.01$). In three of four Sio data sets, correct classification became significant from 0.3 s to 1 s after target onset (Fig. 8*D*; binomial test, $P < 0.01$), suggesting some degree of reliable decoding of the direction of tongue protrusion. This also supports the finding that directional information was available earlier in Sio compared with Mlo.

Decoding of tongue direction using neural data aligned at force onset was highly reliable compared with decoding that used neural data aligned at target onset. Moreover, the temporal evolution of the directional information showed marked differences between neural activities aligned at target onset and those aligned at force onset. This confirms that the neural activity of Mlo and Sio neurons is better time-locked to the force onset compared with the target onset. Finally, classifier

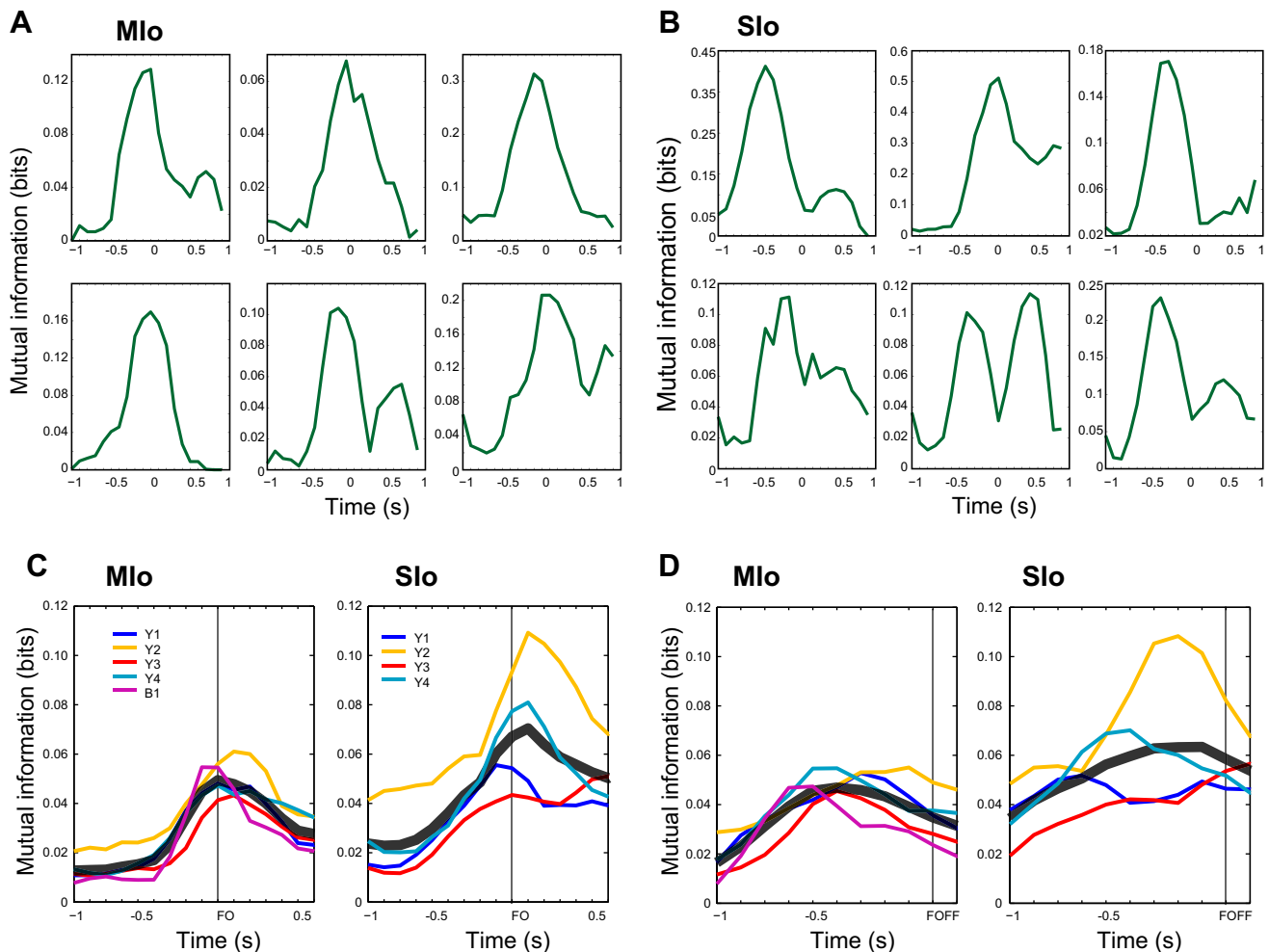


Fig. 6. Mutual information between spiking activity and direction of tongue protrusion. *A* and *B*: temporal profiles of mutual information of representative single neurons in Mlo and Slo exhibit significant modulation of directional information. Shown for data aligned at force onset (0 s) and for single units in Mlo and Slo, respectively. *C*: mean directional mutual information across all Mlo and Slo neurons for each data set aligned at force onset (FO). Thick gray lines denote the mean mutual information across all data sets. Colors correspond to a data set from monkey *Y* (Y1–Y4) or monkey *B* (B1). *D*: as in *C* for data set aligned at force offset (FOFF). Directional mutual information values were corrected for bias.

performance starting 1 s prior to target onset was above chance level particularly in Slo, signifying that some directional information was carried by Mlo and Slo neurons even during the base hold period.

DISCUSSION

In this study, we have shown that directional information is carried by populations of spiking neurons in Mlo and Slo in a parallel and distributed manner when monkeys make voluntary tongue protrusions to different directions. While both cortical sites exhibited significant directional information, encoding and decoding the tongue direction using spiking activity of Mlo and Slo ensembles differed in their temporal evolution.

Concurrent Modulation of Orofacial Motor and Somatosensory Cortices

Previous studies have reported that Mlo and Slo neurons showing tongue protrusion-related activity shared common features such as the proportion of directionally modulated neurons, index of modulation, and directional preference (Lin et al. 1994b; Murray and Sessle 1992c). Our simultaneous

recording from Mlo and Slo revealed important similarities in the tongue-protrusive directional content carried by these cortical areas, confirming some of these previous findings and suggesting parallel and distributed processing of directional information. However, unlike previous studies, we found that the directional index of modulation of Slo neurons was significantly stronger than that of Mlo neurons. The conflicting results between our study and previous ones may be attributed mainly to the different cortical areas sampled within Slo. The nature of the RFs that we identified for most Slo neurons is consistent with RF properties of Slo neurons recorded primarily from area 2 (and to some extent from area 1), which were bilateral, larger, and composite, versus the unilateral, smaller, and discrete RFs described for area 3b (Huang et al. 1989b; Toda and Taoka 2002, 2004, 2006). The RF properties reported by Lin et al. (1994b) corresponded mainly to neurons in areas 3b and 1.

The simultaneous recording from Mlo and Slo in the present study ensured that all other conditions during task performance were identical. Thus any differences noted can be primarily attributed to properties inherent to modulation properties of

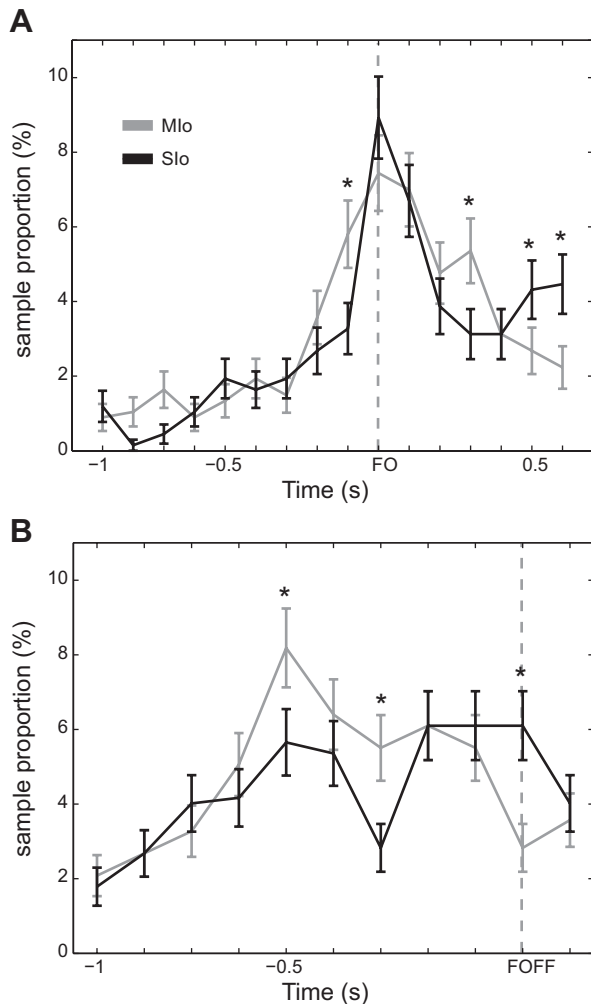


Fig. 7. Population distribution of time-to-peak directional mutual information in MIO and SIO neurons. *A*: binned data (100 ms) aligned at force onset (FO). Data were pooled across all data sets. *B*: as in *A* for data aligned at force offset (FOFF). * $P < 0.05$ (binomial test).

MIO and SIO neurons and suggestive of differences in which directional information is represented in MIO and SIO. The difference in signal-related activity that we observed in both mean firing rates and mutual information may be attributed to the following factors. First, in our study, directionally modulated SIO neurons had RFs that were bilateral, larger, and composite (i.e., including peri- and intraoral structures). Thus, during movement execution, these SIO neurons were likely to receive a greater bulk of input coming from the periphery (e.g., lip area, surrounding teeth) associated with the generation of tongue-protrusive force. This suggests that important sensory information includes not only tongue position and shape but also mechanosensory inputs from surrounding orofacial structures such as when the tongue contacts the lower teeth and lower lip while pressing on the transducer. In contrast, directionally modulated MIO neurons had RFs limited to the tongue and some had peak activity after the force onset. This suggests that part of the directional information in MIO may be attributed to MIO neurons' responses to tongue mechanoreceptors as the tongue moves.

Second, distinct tongue kinematics (see displacements and velocity in Fig. 2*B*) before and during force generation could

account for distinct and relevant sensory inputs to SIO neurons during these epochs. This could lead to activation of different neuronal ensembles within SIO, with the tongue approaching the transducer versus its pressing on the transducer to generate the required force. Indeed, area 2 has been suggested to mediate oral stereognosis and higher somatosensory processing requiring integration of many oral structures (Toda and Taoka 2002, 2004, 2006). Load-sensitive neurons, like those found in the arm region of the primary somatosensory cortex (Jennings et al. 1983; Prud'homme and Kalaska 1994; Wolpaw 1980), are also likely to be present in SIO and thus would have been activated during force generation.

Population Decoding of Tongue Protrusion Direction

Enabled by current available technology to record simultaneously from many neurons from both MIO and SIO, we have shown that the direction of tongue protrusion can be accurately decoded from the spiking activity of populations of MIO and SIO neurons on a trial-by-trial basis. The high reliability of decoding performance was surprisingly similar for MIO and SIO ensembles, indicating that both cortical areas were highly involved in processing directional information required by the tongue protrusion task (Lin et al. 1994b; Murray and Sessle 1992c). However, directional information was available earlier and was sustained in SIO compared with MIO (see Fig. 8). In view of this finding and the documented SIO projection to MIO (Hatanaka et al. 2005; Huang et al. 1989a, 1989b), this may indicate information flow between these two cortical areas. The 200-ms lead time for directional information in SIO suggests that SIO makes directional information available to MIO prior to upcoming movement. In turn, MIO uses directional information to drive the required motor output via its projections to the hypoglossal nuclei to effect changes in tongue position and shape by activating both extrinsic and intrinsic tongue muscles to generate tongue-protrusive force along a specific direction (Kuypers 1960; Lowe 1980; Murray and Sessle 1992a; Sirisko and Sessle 1983). The origin of this early directional information in SIO may be a reflection of set-related activity from the premotor cortex (Grabski et al. 2012; Yoshino et al. 2000). This may allow comparisons between predicted sensory consequences and actual sensory inputs.

The early directional information in SIO may also reflect information flow between SIO and other orofacial cortical areas [e.g., supplementary motor area (SMAo), cortical masticatory area (CMA), secondary somatosensory area (SIIo), and posterior parietal cortex] for sensorimotor processing (Hatanaka et al. 2005; Huang et al. 1989b; Pandya and Kuypers 1969). Cortico-cortical connections between motor and somatosensory cortices have been described in other animal models as well and have been suggested to be critical for sensorimotor integration (Kaneko et al. 1994; Mao et al. 2011; Petreanu et al. 2012). Likewise, there are descending projections from SIO to thalamus or brain stem for modulation of sensory information sent to higher brain centers including SIO itself; these descending modulatory influences appear to underlie a gating or selection of sensory inputs (Chapin and Woodward 1982; Chapman et al. 1988; Haque et al. 2012; Tomita et al. 2012). Indeed, RF afferent inputs to many SIO neurons can be gated out during tongue protrusion, resulting in diminution of short-latency evoked activity in SIO itself (Lin and Sessle 1994).

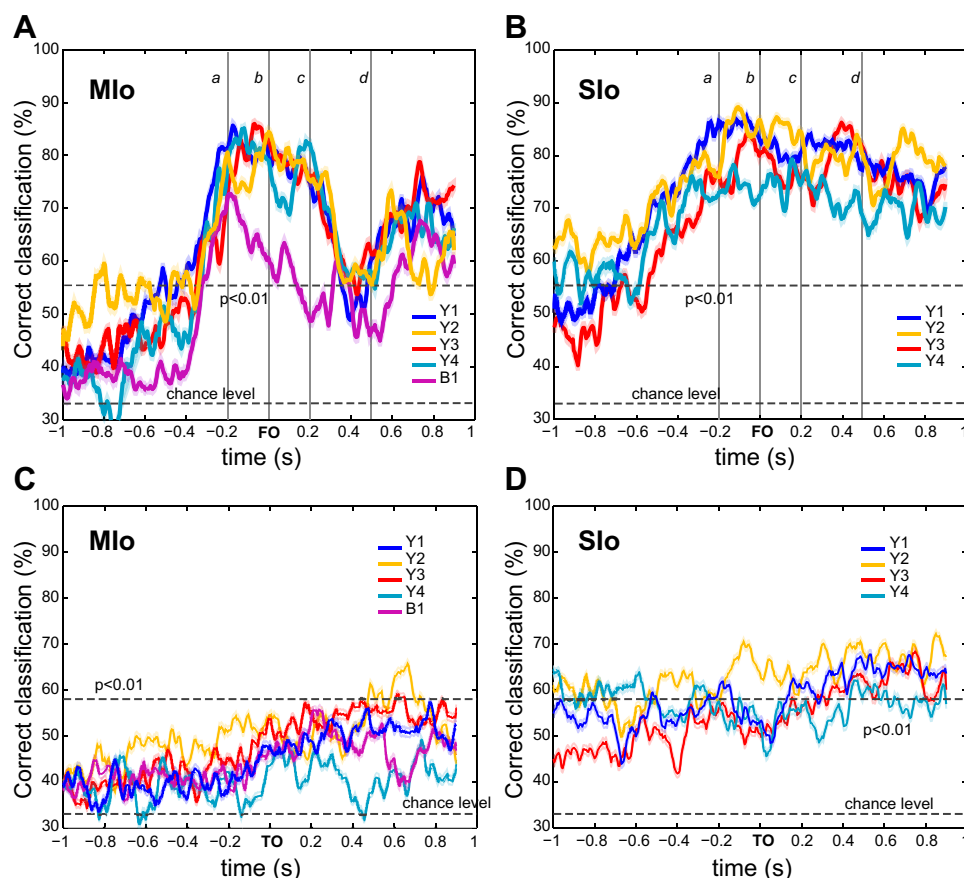


Fig. 8. Decoding the direction of tongue protrusion from single-unit activity. *A* and *B*: plots show average correct performance of a nearest-neighbor classifier (100 runs, ± 1 SE) using population activity aligned at force onset (FO); 5 data sets from Mlo (*A*) and 4 data sets from Slo (*B*). Vertical gray lines mark onset of tongue protrusion (*a*), force onset (*b*), force release (*c*), and force offset (*d*). Colors correspond to a data set from monkey *Y* (Y1–Y4) or monkey *B* (B1). Dashed line corresponds to $P < 0.01$ significance level of correct classification (binomial test) and chance level at 33%. *C* and *D*: as in *A* and *B* for neural activity aligned at target onset (TO).

The sustained versus short-lived directional information in SIo and Mlo, respectively, further supports the differential use of directional information between Mlo and SIo. The sustained directional information in SIo raises the possibility that SIo may provide tongue positional information well beyond force release (Fig. 8*B*, lines *c* and *d*). This also explains the above-chance level performance of the classifier 1 s prior to target onset in SIo (45–65%) but not in Mlo. In contrast, the drop in the directional information in Mlo as soon as the required force was reached (Fig. 8*A*, lines *c* and *d*) implies that Mlo encodes directional information that relates to generating tongue-protrusive force. The ensuing increase in directional information in Mlo after force offset likely corresponded to directional information during tongue retraction.

Strengths and Limitations of Present Study

This study involved the use of chronically implanted micro-electrode arrays, a methodology that has never been applied before to the orofacial sensorimotor cortex. Such a recording technique allowed for simultaneous recording of multiple single neurons in awake and behaving animals and for comparing activity patterns between Mlo and SIo neurons. The results we report from Mlo consist of data sets from two monkeys that showed, across data sets and between monkeys, similar general patterns with regard to rate modulation and decoding properties. While some differences between monkeys can be noted in the amplitude of the decoding performance, important similarities in the temporal profiles were observed between the two monkeys. This is highly suggestive of a pattern for the temporal processing of directional information in populations of

neurons in Mlo. To our knowledge, this is the first study to show decoding properties from neuronal populations from Mlo and SIo. Although the results from SIo were limited to data from one monkey, these results were nevertheless also highly consistent across all our data sets and conformed to those of previous studies (Huang et al. 1989a, 1989b; Lin et al. 1994b; Lin and Sessle 1994). Our SIo neuronal recordings nonetheless were limited to certain areas of SIo, and future studies focusing on SIo will need to address whether the different SIo areas have similar or different encoding and modulation features during orofacial motor behaviors. In addition, while conducting this study in awake animals had the advantage of being able to relate neuronal properties to trained behavior, it did limit our ability to assess fully the features of intraoral RFs, e.g., the presence of an ipsilateral, contralateral, or bilateral lingual RF.

The number of directions that we sampled in this study was limited. Because of this, we were limited to using a discrete decoder. A future research direction is to increase the number of directions and to monitor tongue direction continuously in time so as to decode instantaneous tongue movements.

Conclusions

The directional modulation found in Mlo and SIo neurons here and in previous studies (Lin et al. 1994b; Murray and Sessle 1992c) is akin to that described for motor cortical neurons (Georgopoulos et al. 1982; Kalaska et al. 1989; Schwartz et al. 1988) and somatosensory cortical neurons (Burbaud et al. 1991; Prud'homme and Kalaska 1994; Soso and Fetz 1980) of the arm region. We have shown further that, as in the arm motor cortex and posterior parietal cortex (Geor-

gopoulos et al. 1986; Hatsopoulos et al. 2004; Quian et al. 2006; Shenoy et al. 2003), discrete movement or target direction can be accurately decoded on a trial-by-trial basis from the spiking activity of populations of Mlo and Sio neurons recorded simultaneously during the same directional task.

Our findings provide support for a parallel and distributed processing of directional information by populations of neurons in Mlo and Sio during a voluntary tongue protrusion task. While the task is limited to tongue protrusion, the robust directional decoding supports the view that direction is an important feature of the cortical control of tongue movements in general and that the orofacial motor and somatosensory cortices may differ in their temporal representation of directional information. Overall, our findings show that similar principles govern the representation of effector movement direction in the arm and orofacial regions of the sensorimotor cortex.

ACKNOWLEDGMENTS

We thank Kevin Brown for assistance with data analysis, Meghan Rock for assistance with illustrations, and Josh Coles and Kate Murray for assistance with the experiments.

GRANTS

This work was supported by Canadian Institutes of Health Research (CIHR) Grant MOP-4918.

DISCLOSURES

No conflicts of interest, financial or otherwise, are declared by the author(s).

AUTHOR CONTRIBUTIONS

Author contributions: F.I.A., J.-C.L., C.F.R., B.J.S., and N.G.H. conception and design of research; F.I.A. performed experiments; F.I.A. and N.G.H. analyzed data; F.I.A., C.F.R., B.J.S., and N.G.H. interpreted results of experiments; F.I.A. prepared figures; F.I.A. drafted manuscript; F.I.A., C.F.R., B.J.S., and N.G.H. edited and revised manuscript; F.I.A., J.-C.L., C.F.R., B.J.S., and N.G.H. approved final version of manuscript.

REFERENCES

- Arce F, Hatsopoulos NG, Brown K, Takahashi K, Lee JC, Ross CF, Sessle BJ. Dynamics of modulation in orofacial sensorimotor cortex during long-term adaptation to a novel tongue-protrusion task (Abstract). *Neuroscience Meeting Planner* 2011: 19.02, 2011.
- Arce F, Novick I, Shahar M, Link Y, Ghez C, Vaadia E. Differences in context and feedback result in different trajectories and adaptation strategies in reaching. *PLoS One* 4: e4214, 2009.
- Arima T, Yanagi Y, Niddam DM, Ohata N, Arendt-Nielsen L, Minagi S, Sessle BJ, Svensson P. Corticomotor plasticity induced by tongue-task training in humans: a longitudinal fMRI study. *Exp Brain Res* 212: 199–212, 2011.
- Avivi-Arber L, Martin R, Lee JC, Sessle BJ. Face sensorimotor cortex and its neuroplasticity related to orofacial sensorimotor functions. *Arch Oral Biol* 56: 1440–1465, 2011.
- Brown G, Pocock A, Zhao S, Lujan M. Conditional likelihood maximization: a unifying framework for information theoretic feature selection. *J Mach Learn Res* 13: 27–66, 2012.
- Burbaud P, Doegle C, Gross C, Bioulac B. A quantitative study of neuronal discharge in areas 5, 2, and 4 of the monkey during fast arm movements. *J Neurophysiol* 66: 429–443, 1991.
- Chapin JK, Woodward DJ. Somatic sensory transmission to the cortex during movement: gating of single cell responses to touch. *Exp Neurol* 78: 654–669, 1982.
- Chapman CE, Jiang W, Lamarre Y. Modulation of lemniscal input during conditioned arm movements in the monkey. *Exp Brain Res* 72: 316–334, 1988.
- Ciucci MR, Russell JA, Schaser AJ, Doll EJ, Vinney LM, Connor NP. Tongue force and timing deficits in a rat model of Parkinson disease. *Behav Brain Res* 222: 315–320, 2011.
- Fleming SM, Schallert T, Ciucci MR. Cranial and related sensorimotor impairments in rodent models of Parkinson's disease. *Behav Brain Res* 231: 317–322, 2012.
- Georgopoulos AP, Kalaska JF, Caminiti R, Massey JT. On the relations between the direction of two-dimensional arm movements and cell discharge in primate motor cortex. *J Neurosci* 2: 1527–1537, 1982.
- Georgopoulos AP, Schwartz AB, Kettner RE. Neuronal population coding of movement direction. *Science* 233: 1416–1419, 1986.
- Grabski K, Lamalle L, Vilain C, Schwartz JL, Vallee N, Tropres I, Baci M, Le Bas JF, Sato M. Functional MRI assessment of orofacial articulators: neural correlates of lip, jaw, larynx, and tongue movements. *Hum Brain Mapp* 33: 2306–2321, 2012.
- Haque T, Akhter F, Kato T, Sato F, Takeda R, Higashiyama K, Moritani M, Bae YC, Sessle BJ, Yoshida A. Somatotopic direct projections from orofacial areas of secondary somatosensory cortex to trigeminal sensory nuclear complex in rats. *Neuroscience* 219: 214–233, 2012.
- Hatanaka N, Tokuno H, Nambu A, Inoue T, Takada M. Input-output organization of jaw movement-related areas in monkey frontal cortex. *J Comp Neurol* 492: 401–425, 2005.
- Hatsopoulos N, Joshi J, O'Leary JG. Decoding continuous and discrete motor behaviors using motor and premotor cortical ensembles. *J Neurophysiol* 92: 1165–1174, 2004.
- Huang CS, Hiraba H, Murray GM, Sessle BJ. Topographical distribution and functional properties of cortically induced rhythmical jaw movements in the monkey (*Macaca fascicularis*). *J Neurophysiol* 61: 635–650, 1989a.
- Huang CS, Hiraba H, Sessle BJ. Input-output relationships of the primary face motor cortex in the monkey (*Macaca fascicularis*). *J Neurophysiol* 61: 350–362, 1989b.
- Jennings VA, Lamour Y, Solis H, Fromm C. Somatosensory cortex activity related to position and force. *J Neurophysiol* 49: 1216–1229, 1983.
- Kalaska JF, Cohen DA, Hyde ML, Prud'homme M. A comparison of movement direction-related versus load direction-related activity in primate motor cortex, using a two-dimensional reaching task. *J Neurosci* 9: 2080–2102, 1989.
- Kaneko T, Caria MA, Asanuma H. Information processing within the motor cortex. II. Intracortical connections between neurons receiving somatosensory cortical input and motor output neurons of the cortex. *J Comp Neurol* 345: 172–184, 1994.
- Kennedy D, Kieser J, Bolter C, Swain M, Singh B, Waddell JN. Tongue pressure patterns during water swallowing. *Dysphagia* 25: 11–19, 2010.
- Konaka K, Kondo J, Hirota N, Tamine K, Hori K, Ono T, Maeda Y, Sakoda S, Naritomi H. Relationship between tongue pressure and dysphagia in stroke patients. *Eur Neurol* 64: 101–107, 2010.
- Kuypers HG. Central cortical projections to motor and somato-sensory cell groups. An experimental study in the rhesus monkey. *Brain* 83: 161–184, 1960.
- Lin LD, Murray GM, Sessle BJ. Functional properties of single neurons in the primate face primary somatosensory cortex. I. Relations with trained orofacial motor behaviors. *J Neurophysiol* 71: 2377–2390, 1994a.
- Lin LD, Murray GM, Sessle BJ. Functional properties of single neurons in the primate face primary somatosensory cortex. II. Relations with different directions of trained tongue protrusion. *J Neurophysiol* 71: 2391–2400, 1994b.
- Lin LD, Sessle BJ. Functional properties of single neurons in the primate face primary somatosensory cortex. III. Modulation of responses to peripheral stimuli during trained orofacial motor behaviors. *J Neurophysiol* 71: 2401–2413, 1994.
- Lowe AA. The neural regulation of tongue movements. *Prog Neurobiol* 15: 295–344, 1980.
- Mao T, Kusefoglu D, Hooks BM, Huber D, Petreanu L, Svoboda K. Long-range neuronal circuits underlying the interaction between sensory and motor cortex. *Neuron* 72: 111–123, 2011.
- Martin RE, Kempainen P, Masuda Y, Yao D, Murray GM, Sessle BJ. Features of cortically evoked swallowing in the awake primate (*Macaca fascicularis*). *J Neurophysiol* 82: 1529–1541, 1999.
- Murray GM, Lin LD, Moustafa EM, Sessle BJ. Effects of reversible inactivation by cooling of the primate face motor cortex on the performance

- of a trained tongue-protrusion task and a trained biting task. *J Neurophysiol* 65: 511–530, 1991.
- Murray GM, Sessle BJ.** Functional properties of single neurons in the face primary motor cortex of the primate. I. Input and output features of tongue motor cortex. *J Neurophysiol* 67: 747–758, 1992a.
- Murray GM, Sessle BJ.** Functional properties of single neurons in the face primary motor cortex of the primate. II. Relations with trained orofacial motor behavior. *J Neurophysiol* 67: 759–774, 1992b.
- Murray GM, Sessle BJ.** Functional properties of single neurons in the face primary motor cortex of the primate. III. Relations with different directions of trained tongue protrusion. *J Neurophysiol* 67: 775–785, 1992c.
- Nuckolls AL, Worley C, Leto C, Zhang H, Morris JK, Stanford JA.** Tongue force and tongue motility are differently affected by unilateral vs. bilateral nigrostriatal dopamine depletion in rats. *Behav Brain Res* 234: 343–348, 2012.
- Pandya DN, Kuypers HG.** Cortico-cortical connections in the rhesus monkey. *Brain Res* 13: 13–36, 1969.
- Petreaanu L, Gutnisky DA, Huber D, Xu NL, O'Connor DH, Tian L, Looger L, Svoboda K.** Activity in motor-sensory projections reveals distributed coding in somatosensation. *Nature* 489: 299–303, 2012.
- Prud'homme MJ, Kalaska JF.** Proprioceptive activity in primate primary somatosensory cortex during active arm reaching movements. *J Neurophysiol* 72: 2280–2301, 1994.
- Quian QR, Snyder LH, Batista AP, Cui H, Andersen RA.** Movement intention is better predicted than attention in the posterior parietal cortex. *J Neurosci* 26: 3615–3620, 2006.
- Rousche PJ, Normann RA.** Chronic recording capability of the Utah Intra-cortical Electrode Array in cat sensory cortex. *J Neurosci Methods* 82: 1–15, 1998.
- Schwartz AB, Kettner RE, Georgopoulos AP.** Primate motor cortex and free arm movements to visual targets in three-dimensional space. I. Relations between single cell discharge and direction of movement. *J Neurosci* 8: 2913–2927, 1988.
- Serruya MD, Hatsopoulos NG, Paninski L, Fellows MR, Donoghue JP.** Instant neural control of a movement signal. *Nature* 416: 141–142, 2002.
- Sessle BJ.** Mechanisms of oral somatosensory and motor functions and their clinical correlates. *J Oral Rehabil* 33: 243–261, 2006.
- Sessle BJ, Adachi K, Avivi-Arber L, Lee J, Nishiura H, Yao D, Yoshino K.** Neuroplasticity of face primary motor cortex control of orofacial movements. *Arch Oral Biol* 52: 334–337, 2007.
- Sessle BJ, Yao D, Nishiura H, Yoshino K, Lee JC, Martin RE, Murray GM.** Properties and plasticity of the primate somatosensory and motor cortex related to orofacial sensorimotor function. *Clin Exp Pharmacol Physiol* 32: 109–114, 2005.
- Shannon CE.** A mathematical theory of communication. *Bell Syst Tech J* 27: 379–423, 1948.
- Shenoy KV, Meeker D, Cao S, Kureshi SA, Pesaran B, Buneo CA, Batista AP, Mitra PP, Burdick JW, Andersen RA.** Neural prosthetic control signals from plan activity. *Neuroreport* 14: 591–596, 2003.
- Sirisko MA, Sessle BJ.** Corticobulbar projections and orofacial and muscle afferent inputs of neurons in primate sensorimotor cerebral cortex. *Exp Neurol* 82: 716–720, 1983.
- Soso MJ, Fetz EE.** Responses of identified cells in postcentral cortex of awake monkeys during comparable active and passive joint movements. *J Neurophysiol* 43: 1090–1110, 1980.
- Steele CM, Bailey GL, Molfenter SM, Yeates EM, Grace-Martin K.** Pressure profile similarities between tongue resistance training tasks and liquid swallows. *J Rehabil Res Dev* 47: 651–660, 2010.
- Taylor DM, Tillery SI, Schwartz AB.** Direct cortical control of 3D neuro-prosthetic devices. *Science* 296: 1829–1832, 2002.
- Toda T, Taoka M.** Hierarchical somesthetic processing of tongue inputs in the postcentral somatosensory cortex of conscious macaque monkeys. *Exp Brain Res* 147: 243–251, 2002.
- Toda T, Taoka M.** Converging patterns of inputs from oral structures in the postcentral somatosensory cortex of conscious macaque monkeys. *Exp Brain Res* 158: 43–49, 2004.
- Toda T, Taoka M.** Postcentral neurons with covert receptive fields in conscious macaque monkeys: their selective responsiveness to simultaneous two-point stimuli applied to discrete oral portions. *Exp Brain Res* 168: 303–306, 2006.
- Tomita A, Kato T, Sato F, Haque T, Oka A, Yamamoto M, Ono T, Bae YC, Maeda Y, Sessle BJ, Yoshida A.** Somatotopic direct projections from orofacial areas of primary somatosensory cortex to pons and medulla, especially to trigeminal sensory nuclear complex, in rats. *Neuroscience* 200: 166–185, 2012.
- Wessberg J, Stambaugh CR, Kralik JD, Beck PD, Laubach M, Chapin JK, Kim J, Biggs SJ, Srinivasan MA, Nicolelis MA.** Real-time prediction of hand trajectory by ensembles of cortical neurons in primates. *Nature* 408: 361–365, 2000.
- Wolpaw JR.** Correlations between task-related activity and responses to perturbation in primate sensorimotor cortex. *J Neurophysiol* 44: 1122–1138, 1980.
- Yao D, Yamamura K, Narita N, Martin RE, Murray GM, Sessle BJ.** Neuronal activity patterns in primate primary motor cortex related to trained or semiautomatic jaw and tongue movements. *J Neurophysiol* 87: 2531–2541, 2002.
- Yoshino K, Kawagishi S, Takatsuki Y, Amano N.** Functional properties of the primary motor cortex and ventral premotor cortex in the monkey during a visually guided jaw-movement task with a delay period. *Brain Res* 852: 414–423, 2000.